

Robin Andlauer, Axel Loewe\*, Olaf Dössel and Gunnar Seemann

# Effect of left atrial hypertrophy on P-wave morphology in a computational model

DOI 10.1515/cdbme-2016-0133

**Abstract:** P-wave assessment is frequently used in clinical practice to recognize atrial abnormalities. However, the use of P-wave criteria to diagnose specific atrial abnormalities such as left atrial enlargement has shown to be of limited use since these abnormalities can be difficult to distinguish using P-wave criteria to date. Hence, a mechanistic understanding how specific atrial abnormalities affect the P-wave is desirable. In this study, we investigated the effect of left atrial hypertrophy on P-wave morphology using an *in silico* approach. In a cohort of four realistic patient models, we homogeneously increased left atrial wall thickness in up to seven degrees of left atrial hypertrophy. Excitation conduction was simulated using a monodomain finite element approach. Then, the resulting transmembrane voltage distribution was used to calculate the corresponding extracellular potential distribution on the torso by solving the forward problem of electrocardiography. In our simulation setup, left atrial wall thickening strongly correlated with an increased absolute value of the P-wave terminal force (PTF) in Wilson lead  $V_1$  due to an increased negative amplitude while P-wave duration was unaffected. Remarkably, an increased PTF- $V_1$  has often been associated with left atrial enlargement which is defined as a rather increased left atrial volume than a solely thickened left atrium. Hence, the observed contribution of left atrial wall thickness changes to PTF- $V_1$  might explain the poor empirical correlation of left atrial enlargement with PTF- $V_1$ .

**Keywords:** left atrial abnormalities; left atrial enlargement; left atrial hypertrophy; left atrium; P-wave.

## 1 Introduction

Increasing occurrence of atrial fibrillation (AF) raises the interest in simple measures to detect predictors for AF. Being non-invasive, inexpensive and routinely acquired in clinical practice, P-wave features assessed in the body surface ECG offer a simple measure to gain insight into the atria and, therefore, could recognize atrial abnormalities that are linked to AF. One particular atrial abnormality, which is associated with the risk to develop AF is left atrial enlargement (LAE) [1]. However, ECG-based detection of LAE is discussed controversially as several studies investigating multiple P-wave criteria showed varying results and generally rather poor to moderate correlations to LAE [2–5]. One possible explanation to these divergent findings is that several left atrial abnormalities (LAAbs) such as inter-atrial conduction block, left atrial hypertrophy (LAH) and other disorders can similarly affect the P-wave and are therefore hard to distinguish using P-wave criteria [6]. This however, limits the use of risk stratification for AF using P-wave criteria. Hence, a better understanding of the effect of specific LAAbs on the P-wave is desirable and may lead to better P-wave features to identify AF related LAAbs. In this study, we investigated the effect of LAH on the P-wave in a computation model. Hereby, an *in silico* approach has the advantage of a direct P-wave comparison of different degrees of LAH in the same patient model and therefore offers an investigation of the effect of LAH in a much more controlled environment in contrast to clinical studies.

## 2 Methods

### 2.1 Left atrial hypertrophy

The effect of LAH was investigated in four healthy anatomical models. The models were acquired by manual and automatic segmentation of MRI data and converted to a voxel format as described in earlier work [7]. Each model comprised a high resolution atrial model with an isotropic voxel side length of 0.33 mm and a heterogeneous thorax model with an isotropic voxel side length of 0.40 mm.

\*Corresponding author: Axel Loewe, Institute of Biomedical Engineering, Karlsruhe Institute of Technology (KIT), Kaiserstr. 12, 76128 Karlsruhe, E-mail: publications@ibt.kit.edu

Robin Andlauer, Olaf Dössel and Gunnar Seemann: Institute of Biomedical Engineering, Karlsruhe Institute of Technology, Germany

Gunnar Seemann: Institute for Experimental Cardiovascular Medicine, University Heart Center Freiburg, Bad Krozingen, Freiburg, Germany; and Medical Department, Albert-Ludwigs University, Freiburg, Germany

 © 2016 Axel Loewe et al., licensee De Gruyter.

This work is licensed under the Creative Commons Attribution-NonCommercial-NoDerivs 4.0 License.

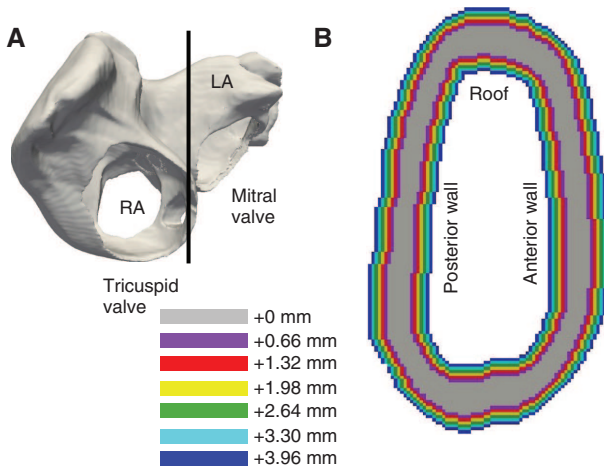


**Figure 1:** (A) shows the left (LA) and right atrium (RA) of model #1 as well as the plane (black line) for the cross section in (B), which shows the seven degrees of LAH in different colors.

In a first step, LAH was applied to the high resolution atria models. To model LAH, the left atrial wall was homogeneously thickened by converting voxels that were adjacent to the left atrium and that did not belong to the right atrium. Hereby, each subsequent degree of LAH was created by adding one voxel layer to left atrial endo- and epicardium, respectively. Therefore, each degree of LAH yielded an additional left atrial wall thickness increase of 0.66 mm. Using this method, seven degrees of LAH with a maximum additional left atrial wall thickness of 3.96 mm were created for each of the four models. Figure 1 shows a cross section of the seven different hypertrophic degrees in model #1. To account for atrial tissue heterogeneities and myocyte orientation, a semi-automatic rule-based algorithm was applied [8]. The algorithm annotated tissue heterogeneities and myocyte orientation along predefined paths by manually defining 22 seed points on the atria models. As the algorithm was robust against atrial wall thickness deviations, path points were set identically for all seven degrees of LAH in each patient model. To enable left atrial activation, four inter-atrial connections were added: Bachmann's Bundle, a connection at the coronary sinus and two posterior connections. In a next step, the hypertrophic atria models were transferred to the corresponding thorax models. Since the resolution of the thorax models was coarser, the voxels were labeled by nearest neighbor interpolation. Hereby, separation between left and right atrium was ensured except for inter-atrial connections. Furthermore, atrial myocyte orientation was transferred to the torso models. Lastly, the voxel-based thorax models were converted to tetrahedral meshes using the CGAL library [9].

## 2.2 Electrophysiological modeling

Cardiac single cell behaviour was described using the model by Courtemanche et al. [10]. Cellular steady state conditions were ensured by initializing single cells for each tissue over 60 cycles. To initialize atrial depolarization, a stimulus current was applied to the sinus node for 3 ms. To account for atrial tissue heterogeneities and myocyte orientation, anisotropy factors and heterogeneous intracellular conductivities were used as described in [11]. Excitation propagation was simulated using a monodomain approach in the reaction-diffusion solver *acCELLerate* [12] by constant time stepping of  $20\mu\text{s}$  for 200 ms. Subsequently, the resulting  $V_m$  distribution was transferred to the corresponding extracellular potential  $\Phi_e$  on the body surface by solving the forward problem of electrocardiography:

$$\nabla \cdot (\sigma_i \nabla V_m) = -\nabla \cdot ((\sigma_i + \sigma_e) \nabla \Phi_e), \quad (1)$$

with  $\sigma_i$  being the intracellular conductivity tensor and  $\sigma_e$  being the extracellular conductivity tensor. In a last step, the twelve-lead ECG was assessed from the extracellular potential map on the body surface.

## 2.3 P-wave analysis

To analyze the effect of LAH on P-wave morphology, we investigated four P-wave criteria that were mentioned to be correlated to either LAE or LAAb in clinical studies [2–6]: An increased negative area of the P-wave terminal force in  $V_1$  (PTF- $V_1$ ), a prolonged P-wave duration (PWD), an increased P-wave area in Einthoven lead II (PW-Area) and a decreased P-wave axis (PW-Axis). PTF- $V_1$  was defined as the product of the amplitude and the duration of the terminal negative P-wave component. PW-Area was approximated by 0.5 times duration times amplitude as described in [5]. PW-Axis  $\alpha$  was estimated by the amplitude of Goldberger lead aVF and Einthoven lead I:

$$\alpha = \arctan \left( \frac{2}{\sqrt{3}} \frac{aVF}{I} \right). \quad (2)$$

## 3 Results

The presented method to thicken the left atrial myocardium was applied to four patient models for seven different degrees of LAH. However, tetrahedral torso meshes could not be derived from the voxel based torsos in 8 of

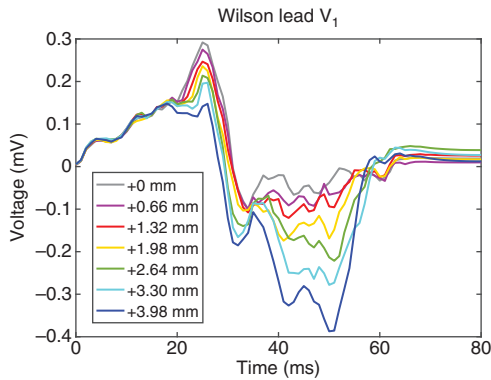


**Figure 2:** P-waves of the seven degrees of LAH in Wilson lead  $V_1$  in model #1.

28 cases using CGAL. Therefore, P-waves were not considered for these eight cases. In our simulation setup, PTF- $V_1$  showed the best correlation with LAH with correlation coefficients ranging from  $-0.88$  to  $-0.99$ . To illustrate the effect of LAH on PTF- $V_1$ , Figure 2 shows the P-waves in Wilson  $V_1$  for all seven degrees of LAH in model #1. For the first 20 ms, P-wave morphology was almost unaffected by left atrial wall thickening as the left atrium was not yet activated. Then, increasing left atrial wall thickness caused a negative deflection of the P-wave resulting both in a smaller positive amplitude and a more pronounced negative amplitude. Thus, the negative amplitude in  $V_1$  correlated even stronger with LAH ranging from  $-0.95$  to  $-1$ . As seen in Figure 3B, PWD hardly varied for different degrees of left atrial wall thickening in the same model with regression slopes ranging from 0 ms per millimeter wall thickening to 1 ms per millimeter wall thickening. PW-Area increased with additional LAH in most cases as a result of an increased amplitude with correlation coefficients ranging from 0.05 to 0.9 (Figure 3C). As seen in Figure 3D, the effect of left atrial wall thickening on PW-Axis was highly model dependent. For model #1 and #2, PW-Axis correlation was positive while model #3 and #4 showed negative correlation with LAH.

## 4 Discussion

Our results suggest that increased left atrial wall thickness is reflected in a negative deviation of the terminal P-wave in  $V_1$  resulting in an increased absolute value of PTF- $V_1$ . Furthermore, we conclude that left atrial wall thickness does not affect PWD and potentially affects PW-Area in Einthoven II and PW-Axis depending on anatomical properties of the patient. Although our virtual population of

four patients was small compared to most *in vivo* studies, an *in silico* approach carries the advantage of solely altering specific anatomical properties in the same patient. Hence, the presented approach to thicken the left atrial wall allows to draw conclusions in a much smaller study population compared to clinical studies. However, we modeled LAH by assuming left atrial wall thickness to be homogeneous and limited to the left atrium, which might not be the case *in vivo*. Moreover, the wall thickness difference between the chosen seven degrees of LAH might have been too large as in particular the first degree of LAH already thickened the left atrial wall by 20%. An increased absolute PTF- $V_1$  has often been associated with the presence of LAE in clinical studies [3, 4]. Hence, the observed strong correlation of LAH with PTF- $V_1$  raises the interest how LAH contributes to LAE. Generally, LAE is rather defined as an increased left atrial volume than an increased left atrial wall thickness. Nevertheless, LAH could be present during the formation of LAE as it is known for the dilation of ventricles due to pressure overload [13]. Hereby, the left ventricle adapts to high blood pressure by increasing the myocardial thickness (compensation). If the blood pressure further increases, the ventricle dilates (decompensation). Assuming a similar course for LAE, PTF- $V_1$  would increase during the compensation phase due to left atrial wall thickening. Once dilation sets in, PTF- $V_1$  would decrease due to a thinner left atrial myocardium. Conceptually, the decrease of PTF- $V_1$  during the decompensation phase could be counteracted by a prolongation of the P-wave as an effect of left atrial dilation. This could explain the strong correlations of LAE with PWD and the poor correlations with PTF- $V_1$  observed in [5]. In conclusion, we found PTF- $V_1$  to be strongly correlated to left atrial wall thickening while PWD was unaffected. Moreover, the contribution of left atrial wall thickness changes to LAE might explain the poor performance of PTF- $V_1$  to diagnose LAE in clinical studies.

### Author's statement

**Research funding:** The author state no funding involved. **Conflict of interest:** Authors state no conflict of interest. **Material and Methods:** Informed consent: Informed consent has been obtained from all individuals included in this study. **Ethical approval:** The research related to human use complies with all the relevant national regulations, institutional policies and was performed in accordance with the tenets of the Helsinki Declaration, and has been approved by the authors' institutional review board or equivalent committee.

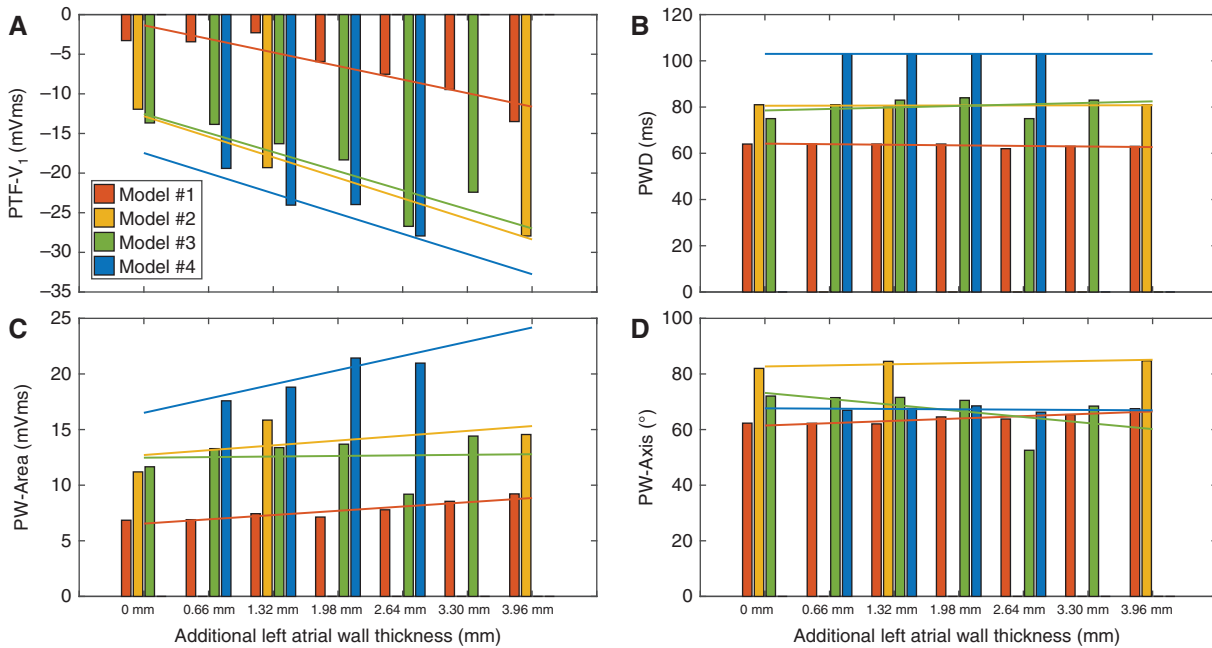


**Figure 3:** Effect of LAH on PTF-V<sub>1</sub>, PWD, PW-Area and PW-Axis. The annotated values of the P-wave criteria are shown for the four anatomical models. Additionally, linear regression lines are shown for each model. Missing values are due to failure of torso mesh generation.

## References

- [1] Henry WL, Morganroth J, Pearlman AS, Clark CE, Redwood DR, Itscoitz SB, et al. Relation between echocardiographically determined left atrial size and atrial fibrillation. *Circulation* 1976;53:273–9.
- [2] Agarwal A, Tsao CWL, Josephson M, O'Halloran TD, Agarwal A, Manning WJ, et al. [Accuracy of electrocardiographic criteria for atrial enlargement: validation with cardiovascular magnetic resonance](#). *J Cardiovasc Magn Reson*. 2008;10:1–7.
- [3] Hazen MS, Marwick TH, Underwood DA. Diagnostic accuracy of the resting electrocardiogram in detection and estimation of left atrial enlargement: an echocardiographic correlation in 551 patients. *Am Heart J*. 1991;122:823–8.
- [4] Alpert MA, Munuswamy K. Electrocardiographic diagnosis of left atrial enlargement. *Arch Intern Med*. 1989;149:1161–5.
- [5] Truong QA, Charipar EM, Ptaszek LM, Taylor C, Fontes JD, Kriegel M, et al. [Usefulness of electrocardiographic parameters as compared with computed tomography measures of left atrial volume enlargement: from the ROMICAT trial](#). *J Electrocardiol*. 2011;44:257–64.
- [6] Hancock EW, Deal BW, Mirvis DM, Okin P, Kligfield P, Gettes LS, et al. AHA/ACCF/HRS recommendations for the standardization and interpretation of the electrocardiogram: Part V. *J Am Coll Cardiol*. 2009;53:992–1002.
- [7] Krueger MW, Seemann G, Rhode K, Keller DU, Schilling C, Arujuna A, et al. Personalization of atrial anatomy and electrophysiology as a basis for clinical modeling of radio-frequency ablation of atrial fibrillation. *IEEE Trans Med Imaging*. 2013;32:73–84.
- [8] Wachter A, Loewe A, Krueger M, Dössel O, Seemann G. Mesh structure-independent modeling of patient-specific atrial fiber orientation. *Curr Dir Biomed Eng*. 2015;1:409–12.
- [9] The CGAL Project, CGAL User and Reference Manual. CGAL Editorial Board; 2015; 4.7 ed.
- [10] Courtemanche M, Ramirez RJ, Nattel S. Ionic mechanisms underlying human atrial action potential properties: insights from a mathematical model. *Am J Physiol*. 1998;275:H301–21.
- [11] Loewe A, Krueger MW, Platonov PG, Holmqvist F, Dössel O, Seemann G. Left and right atrial contribution to the P-wave in realistic computational models. In: *Functional Imaging and Modeling of the Heart*; 2015: Lect Notes Comput Sc; 2015. p. 439–47.
- [12] Seemann G, Sachse FB, Karl M, Weiss DL, Heuveline V, Dössel O. Framework for modular, flexible and efficient solving the cardiac bidomain equations using PETSc. *Math Indust*. 2010;15:363–9.
- [13] Schmidt RF, Lang F, Heckmann M, editors. *Physiologie des Menschen: mit Pathophysiologie*. Springer–Lehrbuch. Heidelberg: Springer; 2010. ISBN 978-3-642-01650-9.